COMMUNICATION

Check for updates

Flexible strain sensors based on silver nanowires and UV-curable acrylate elastomers for wrist movement monitoring†

Shuhao Li,[a] Wenjin Wu,[a] Yu Chang,[a] Weiquan Chen,[a] Yijie Liu,[a] Zifeng He,[a] Yan Pu, [iD][a] Ivan S. Babichuk, [iD]*[ab] Terry Tao Ye,[c] Zhaoli Gao [iD][de] and Jian Yang [iD]*[a]

Flexible strain sensors have a wide range of electronic skin and health monitoring applications. In this paper, flexible strain sensors with unique direction designs were prepared using silver nanowires (AgNWs) and UV-curable acrylate elastomer films. They show an extensive strain range (tensile strain >50%), sensitivity up to 97 of gauge factor, and good reproducibility of up to 10% strain under cyclic tensile tests. The parallel and perpendicular placement of the sensors to strain direction allows us to detect wrist movement in a 360-degree direction with high accuracy.

Flexible strain sensors have great potential for applications in personalized health monitoring,[1] robotics,[2] and pressure sensing.[3] Sensitive, highly stretchable strain sensors can be attached to human skin to monitor pulse, heartbeat, blood pressure, muscle movement, vocalization, and facial expression.[4] Flexible or stretchable sensors can be directly applied to the skin surface and combined with clothes,[5] of which are highly adaptive. In addition, due to their simple preparation process and low cost, wearable sensors based on nanomaterials become one of the current research hotspots in the field of flexible electronics.[6,7] Nanomaterials such as silver nanowires (AgNWs),[8] carbon nanotubes,[9] and graphene[10] have been widely investigated in flexible strain sensors; the working

principle originates from the variation of resistance R under deformation. Upon stretching, the increase in resistance is ascribed to several aspects, including the breakup of the conductive pathway, the loss of contact between neighboring nanomaterials, and the increase in the distance. Current investigations are focused on the design of the sensors, as well as sensitivity (or gauge factor (GF)) and stretchability.[11–14] The sensitivity/GF is quantified as the instant ratio of the relative change in electrical resistance to the applied strain.[15–17] The GF value can significantly differ based on the active materials, assembled structures, and the piezoresistive mechanism used. It is beneficial to enable significant connection or structural modifications to achieve heightened sensitivity, even with minimal strain. Regarding this connection, studies in ref. 18 and 19 have focused on crack-assisted resistive strain sensors, along with the geometric modulation of the elastomer substrate.[8]

Elastic polymer is one of the effective materials utilized as a substrate[20] or capsulation layer[3,21] of flexible sensors. Compared to traditional polymers, including polyethylene terephthalate, polyethylene naphthalate, polyimide, polymethyl methacrylate, *etc.*,[22] to improve the mechanical properties of wearable sensors, it is essential to use a flexible substrate that is also flexible and biocompatible.[23,24] Meanwhile, AgNWs have been extensively utilized to create transparent, flexible, and stretchable strain sensors by embedding them in elastomeric substrates.[25] Previous investigations have shown the importance of generating a uniform conductive layer of AgNWs with high density. This can be achieved by controlling the concentration and amount used during various coating processes, including spin coating, drop casting and ink-jet printing.[26]

Herein, we reported an alternative way for low-cost fabrication of flexible strain sensors using AgNWs with three UV-curable acrylate copolymer films. We expected that by controlling the features of a flexible substrate, an uneven extension of AgNWs would occur upon tension, leading to a significant effect on the GF. Scanning electron microscopy (SEM), and Raman and ATR-FTIR spectroscopy were used to examine the morphology and structure of a new light-cured

[a] *School of Mechanical and Automation Engineering, and Jiangmen Key Laboratory of Intelligent Manufacturing of Polymer Materials, Wuyi University, Jiangmen 529020, Guangdong, P.R. China. E-mail: jiany@szu.edu.cn*

[b] *V. Lashkaryov Institute of Semiconductor Physics, NAS of Ukraine, Kyiv 03680, Ukraine. E-mail: babichuk@isp. kiev.ua*

[c] *Department of Electrical and Electronic Engineering, and University Key Laboratory of Advanced Wireless Communications of Guangdong Province, Southern University of Science and Technology, Shenzhen, 518055, P.R. China*

[d] *Biomedical Engineering Department, The Chinese University of Hong Kong, Shatin, New Territories, Hong Kong, 999077, P.R. China*

[e] *CUHK Shenzhen Research Institute, Nanshan, Shenzhen, 518060, P.R. China*

© 2024 The Author(s). Published by the Royal Society of Chemistry

acrylate elastomer. The piezoresistive characteristic of the sensors was determined by monitoring the output resistance at strain stretching. In addition, the application of the developed sensors for wrist movement monitoring was demonstrated.

Two acrylate monomers, dodecyl acrylate (LA) marked as L, and 4-hydroxybutyl acrylate (4-HBA) as B, were mixed in different volume ratios of 6:4, 5:5, and 4:6, then added 1.5% volume of photoinitiator 1173, respectively. According to the volume proportion of LA and 4-HBA in their respective solutions, they were named L4B6, L5B5, and L6B4. The mixed solution was injected into the mold with a silicone sheet and cured under 365 nm ultraviolet (UV) light (365 nm, Shenzhen, China) with a light intensity of 18.5 mW cm^{-2} for 30 s. After cooling, the film was taken, covered with FEP release films, and vacuumed for 12 h to obtain uniform acrylate copolymer elastomer films.

The preparation process of AgNWs@acrylate copolymer sensors is shown in Fig. 1 and described in the ESI† (material and methods). A transfer "printing" mask prepared the patterned AgNWs on acrylate flexible substrates. Methods of characterization and strain sensitivity of sensors were described in the ESI.† The chemical structures of two acrylate copolymers and their reaction are shown in Fig. 2(a). The SEM morphology of the flexible substrate L6B4, L5B5 and L4B6 films are shown in Fig. 2(b). The surface of the acrylate films had a cross-woven shape, which increased the contact area. Due to this form, there was increased interconnection between AgNWs and the substrate surface, which prevents the AgNWs from falling off easily during the stretching process.

The stress–strain curves and elastic modulus (inset) of the L6B4, L5B5, and L4B6 films are shown in Fig. 2(c). These acrylate films were stretched more than three times their length, and all have good linearity within 300% of the tensile
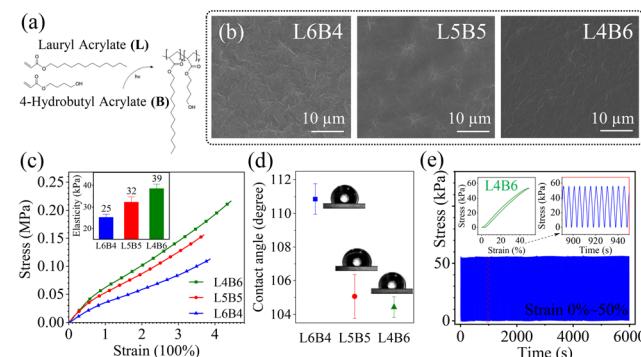

Fig. 2 Performance analysis of acrylate copolymer films. (a) Chemical structure and the reaction of acrylate binary polymers. (b) The SEM morphology of the flexible substrate films: L6B4, L5B5, and L4B6. (c) Uniaxial tensile stress–strain curve and (inset) elastic modulus, (d) the contact angles of acrylate copolymer films. (e) The stretching/releasing cycling test and (inset) the stress–strain hysteresis curve for representative L4B6 film.

strain. Compared with the conventional PDMS substrate, these three elastomer films were more flexible, with an elastic modulus of 25.2 kPa, 32.3 kPa, and 38.6 kPa, respectively (Fig. 2(c, inset)). Their elastic modulus is two orders of magnitude smaller than PDMS (which has an elastic modulus of about 1 MPa),[27] and their mechanical flexibility is closer to human skin (Young's modulus of about 50 kPa).[28] Meanwhile, these acrylate films are transparent and can be easily prepared in different shapes or sizes according to demand. Since flexible strain sensors should have good flexibility and stretchability and require a certain feedback force, the L4B6 film was more suitable as flexible sensor substrates. Fig. 2(d) shows the results of the three acrylate copolymer films' water contact angle tests. The contact angles of L6B4, L5B5 and L4B6 elastomer substrates were 110.86°, 105.33° and 104.43°, respectively, which indicates that changing the monomer ratio will cause the surface activation energy of acrylate copolymers to change. Those acrylate elastomers exhibit hydrophobic properties, similar to the water contact angle of PDMS (from 110–124° to ~91°).[29] A more hydrophobic surface means less roughness, which means better water resistance. These parameters of an elastomer film are crucial for the uniform coating of nanomaterials (in our case, AgNWs) and are directly related to the performance of the sensors. Fig. 2(e) shows the stretching/releasing cycling test near 50% strain and the tensile speed ~0.1 mm s^{-1}. The stress–strain hysteresis curve is shown for a representative L4B6 film. The results confirm high reproducibility for more than 1000 cycles.

Fig. S1† shows the investigation of the structure and functional groups of acrylate copolymer elastomers (ATR FTIR and Raman spectra). The influence of the different monomer ratios on side chains and functional groups was analyzed. The findings, as presented in Fig. S2,† are a supplement to the data in Fig. 2(c and d) and offer a systematic analysis of the mechanical properties associated with the sensor sensitivity (Fig. 3(a)).
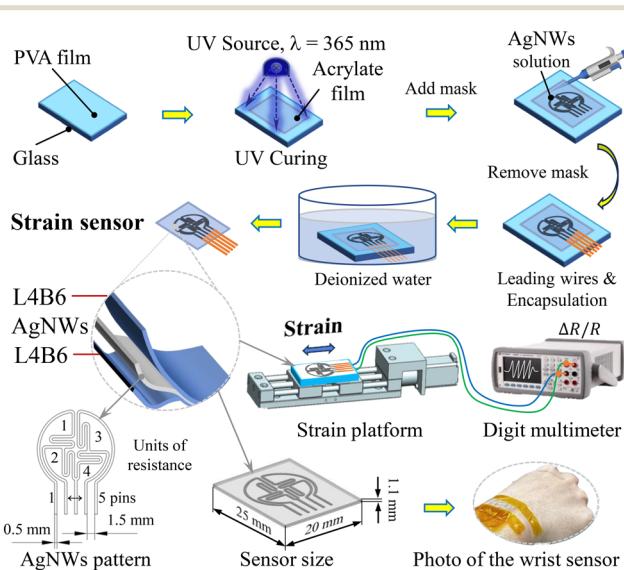

Fig. 1 Preparation of the flexible strain sensors and their structure, size and application.

© 2024 The Author(s). Published by the Royal Society of Chemistry

*RSC Appl. Interfaces*, 2024, **1**, 684–688 | **685**
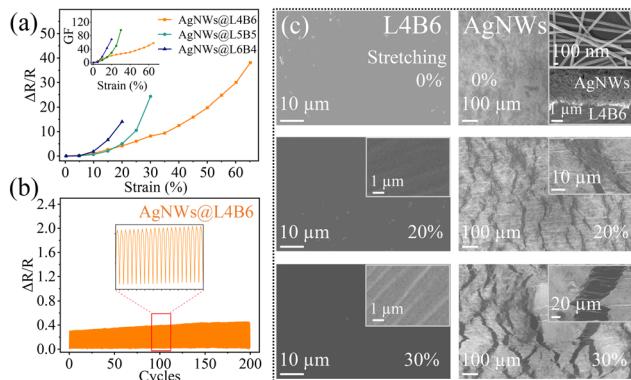
Fig. 3 (a) Relationship between relative resistance variation and strain for sensors with different substrates, (inset) the gauge factor of sensors. (b) The stretching/releasing tests of the representative AgNWs@L4B6 sensors under a cyclic strain of 10%. (c) The SEM morphology of acrylate copolymer film and AgNWs on L4B6 at varied stretching.

The tensile test was performed on AgNWs@L4B6, AgNWs@L5B5 and AgNWs@L6B4 strain sensors and the relationship curves between tensile strain and the rate of change of resistance $\Delta R/R_0$ are shown in Fig. 3(a). The value of the relative change of resistance increases and based on AgNWs@L4B6, the strain sensor sensing range can reach 50% or even greater. The other two AgNWs@L5B5 and AgNWs@L6B4 sensors showed sensitivity with increasing load in the range of up to 30% and 20%, respectively.

The sensitivity (GF) was expressed as the ratio between the relative change in resistance and the applied tensile strain:[30]

$$\mathrm{GF} = \frac{(R - R_0)/R_0}{(L - L_0)/L_0} = \frac{\Delta R/R_0}{\varepsilon} = \frac{\Delta R}{R_0 \varepsilon} \tag{1}$$

where R_0 corresponds to the initial resistance, R refers to the current measured resistance value, ε is the tensile strain, L_0 is the original length of the strain sensor and L refers to the current stretched length. Table S1† shows the relative values of the length of each sensor element (units shown in Fig. 1). The trend of the sensitivity curve in Fig. 3(a, inset) shows that the sensitivity increases with the degree of tensile strain. To evaluate the sensitivity of the strain sensors, the parameter of linearity (R^2) is often used. If this linearity is still around $R^2 \approx 1$, the sensor has a high-quality factor. In our case, the sensitivity and linearity of the AgNWs@L4B6 sensor were GF = 27 ($R^2 \approx 97$) and GF = 58 ($R^2 \approx 98$) in the range of strain tension from 0% to 30% and 30% to 65%, respectively. When the AgNWs@L5B5 sensor was stretched to 15%, the sensitivity was GF = 18 and the linearity was $R^2 \approx 83\%$ with a continued increase in tension to ~25%, the GF of the sensor rising to 97 with linearity $R^2 \approx 88\%$. For the AgNWs@L6B4 sensor from 0% to 10% tensile strain, GF = 19 ($R^2 \approx 78$) and between 10–20% tensile strain, GF = 70 ($R^2 \approx 98$). The sensor shows good linearity in different feature areas, and the linearity of the fitting is basically above 97%. So, the degree of the rise of the GF of the sensors is inconsistent in the different stages of strain, which is mainly because the

different tensile strain leads to changes in the arrangement of AgNWs and the interaction between AgNWs and copolymer substrate. Fig. 3(b) shows the representative sensor's stretching/releasing cycling test 200 times between 0% and 10% strain with the tensile speed at 0.1 mm s⁻¹. Compared to some reported flexible strain sensors (Table S2†), the strain sensors in this work exhibited good sensitivities at maximum strain due to the innovation of UV-curable substrates.

Due to the cracks (breaks) in the conductive path shown in Fig. 3(c) and described in the ESI† (strain analysis of the L4B6 acrylate copolymer film and AgNWs, Fig. S3†),[31] during the stretching process, the sensor's initial resistance value at each stage of the load and unload cycle does not match that value.[32] So $\Delta R/R_0$ also drifted upward with the increase in the number of cycles. This increase in relative resistance is not significant in the short term, as shown in the insets for each sensor, but has an upward trend throughout the test.

By designing the strain sensor as four grids with parallel and perpendicular placements relative to each other (Fig. 4(a)), the sensors are highly selective for the change of strain direction.[33] According to the parameters of the stretching/releasing cycling test near 10% load and the tensile speed ~0.1 mm s⁻¹, the relative resistance $\Delta R/R_0$ of the representative AgNWs@L4B6 strain sensor was measured for different directions of the contact grid and strain directions. The measurement results
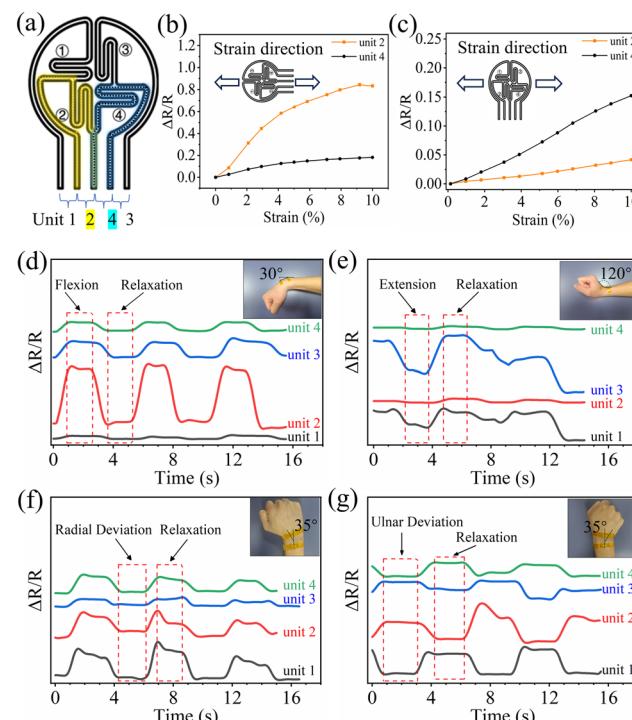
Fig. 4 (a) Schematic diagram of the flexible strain sensor electrodes. Resistive response of the sensor under the parallel (b) and the perpendicular (c) stretching direction to AgNW pin electrodes. Relative resistance changes of a parallel and perpendicular unit of sensor regarding strain directions during wrist flexion (d), extension (e), radial (f) and ulnar (g) deviation.

686 | *RSC Appl. Interfaces*, 2024, **1**, 684–688

© 2024 The Author(s). Published by the Royal Society of Chemistry

show that the relative resistance change $\Delta R/R_0$ of the parallel grid element to the direction strain was higher than $\Delta R/R_0$ of the perpendicular grid element to the strain direction (Fig. 4(b) and (c)). For the sensor stretched along the direction parallel to the strain direction, the load led to a significant response $\Delta R/R_0$. On the other hand, the sensor showed a small response for strain in the perpendicular direction. This directional resistance variation originated from the fact that the resistance change was proportional to the length of the AgNW electrodes in the strain direction. The short length in the perpendicular direction means that the perpendicular strain had less impact on the total resistance of the sensor, whereas the parallel direction strain could cause large resistance to change quickly.[33] The correlations between experimental data and simulation (Fig. S4) are further discussed in the ESI,† shedding light on the underlying mechanism. In this regard, Table S1† shows the relative values of the resistance of each section without stretching. A comparison of elongation at break and strength for the AgNWs@L4B6 strain sensor with different AgNW concentrations is shown in Fig. S5.†

To prove the feasibility of our development design, the AgNWs@L4B6 strain sensor was mounted for the human wrist to detect the uniaxial bending and multiaxial motions. First, the measurements were performed between pins 1 and 5 (Fig. S6†), which includes all the resistors (units 1–4 – Fig. 4(a)). The measurements demonstrated the sensitivity of the sensor to hand movement. However, the value of the change in resistance differed between the bending of the sensor (the hand moved up or down relative to the wrist) and the radial deviation (the hand moved left or right relative to the wrist). Second, the measurements were performed between everything in units 1–4 of the sensor. Fig. 4(d–g) shows these results, where unit 2 and unit 3 parallel to the direction of motion have higher resistance changes than unit 1 and unit 4 perpendicular to the direction of motion under the movements of wrist flexion and wrist extension, respectively. This way, the wrist's deviation and extension can be distinguished according to this change. Thus, the sensor is prominent in detecting wrist movements of flexion, extension, ulnar and radial degrees of freedom. It can be assumed that all 360° movements can be detected this way.

Conclusions

In this article, a flexible strain sensor with good flexibility and stretchability was prepared by using AgNWs and acrylate film. The flexible strain sensors based on AgNWs@L5B5 and AgNWs@L6B4 showed higher strain sensitivity factors GF = 97 and GF = 70, respectively. However, they have a limited stretch range of up to 25% and the lowest parameter of linearity R^2, therefore wrist movement monitoring was shown for the AgNWs@L4B6 sensor with sensitivity GF = 58 at strain 68% and $R^2 \sim 98$. The four grids on the sensor are designed to detect wrist movements in various directions selectively. The sensor can also detect knee bending and finger tapping motion.

Author contributions

Shuhao Li and Jian Yang: conceptualization, Wenjin Wu: methodology, Weiquan Chen: software, Shuhao Li and Yu Chang: validation, Yijie Liu and Zifeng He: formal analysis, Yan Pu and Wenjin Wu: investigation, Shuhao Li: writing – original draft preparation, Ivan S. Babichuk and Jian Yang: writing – review and editing, Shuhao Li visualization, Terry Tao Ye, Zhaoli Gao and Jian Yang: funding acquisition.

Conflicts of interest

There are no conflicts to declare.

Acknowledgements

Notes and references

1 M. Ali, S. M. Hoseyni, R. Das, M. Awais, I. Basdogan and L. Beker, *Adv. Mater. Technol.*, 2023, **8**, 2300347.

2 L. Wang, F. Wei, Z. Zhai, R. Zhang, W. Liu and Z. Zhao, *Sens. Actuators, A*, 2024, **365**, 114909.

3 C. Lin, W. Wu, H. Zhu, Y. Qiu, S. Cui, W. Chen, I. S. Babichuk, T. T. Ye, Z. Gao and J. Yang, *Adv. Mater. Technol.*, 2023, **8**, 2202142.

4 J. Chen, Y. Zhu, X. Chang, D. Pan, G. Song, Z. Guo and N. Naik, *Adv. Funct. Mater.*, 2021, **31**, 2104686.

5 J. Yang, *Front. Bioeng. Biotechnol.*, 2022, **10**, 849617.

6 J. Gu, Y. Shen, S. Tian, Z. Xue and X. Meng, *Biosensors*, 2023, **13**, 1025.

7 F. Basarir, Z. Madani and J. Vapaavuori, *Adv. Mater. Interfaces*, 2022, **9**, 2200866.

8 Y. Heo, Y. Hwang, H. S. Jung, S. H. Choa and H. C. Ko, *Small*, 2017, **13**, 1700070.

9 H. Wang, M. Jian, S. Li, X. Liang, H. Lu, K. Xia, M. Zhu, Y. Wu and Y. Zhang, *Adv. Mater.*, 2023, **35**, 2306144.

10 Q. Liu, J. Chen, Y. Li and G. Shi, *ACS Nano*, 2016, **10**, 7901–7906.

11 B. Chen, L. Zhang, H. Li, X. Lai and X. Zeng, *J. Colloid Interface Sci.*, 2022, **617**, 478–488.

12 A. K. Tareen, K. Khan, M. Iqbal, S. Golovynskyi, Y. Zhang, A. Mahmood, N. Mahmood, J. Long, A. Al-Ghamdi, C. Li and H. Zhang, *Mater. Today Chem.*, 2022, **26**, 101205.

13 K. K. Yeung, J. Li, T. Huang, I. I. Hosseini, R. Al Mahdi, M. M. Alam, H. Sun, S. Mahshid, J. Yang, T. T. Ye and Z. Gao, *Nano Lett.*, 2022, **22**, 6647–6654.

14 X. Yang, H. Yao, G. Zhao, G. A. Ameer, W. Sun, J. Yang and S. Mi, *J. Mater. Sci.*, 2020, **55**, 9551–9561.

15 T. Yang, D. Xie, Z. Li and H. Zhu, *Mater. Sci. Eng., R*, 2017, **115**, 1–37.

© 2024 The Author(s). Published by the Royal Society of Chemistry

RSC Appl. Interfaces, 2024, **1**, 684–688 | **687**

16 Z. Liu, D. Qi, P. Guo, Y. Liu, B. Zhu, H. Yang, Y. Liu, B. Li, C. Zhang, J. Yu, B. Liedberg and X. Chen, *Adv. Mater.*, 2015, **27**, 6230–6237.

17 J. Wang, H. Liu, X. Yue, D. Zhang, R. Yin, H. Sun, C. Liu and C. Shen, *Mater. Today Nano*, 2023, **24**, 100427.

18 C. Wang, J. Zhao, C. Ma, J. Sun, L. Tian, X. Li, F. Li, X. Han, C. Liu, C. Shen, L. Dong, J. Yang and C. Pan, *Nano Energy*, 2017, **34**, 578–585.

19 S. Chen, Y. Wei, S. Wei, Y. Lin and L. Liu, *ACS Appl. Mater. Interfaces*, 2016, **8**, 25563–25570.

20 W. Chen, Y. Qiu, I. S. Babichuk, Y. Chang, R. Zhou, Z. He, Y. Liu, J. Zhang, I. V. Babichuk, A. Tiutiunnyk, D. Laroze, V. V. Brus and J. Yang, *Adv. Eng. Mater.*, 2023, **26**, 2301470.

21 Z. He, Y. Liu, I. S. Babichuk, Z. Zhou, Z. Liu, X. Yang, R. Zhou, Y. Pu, S. Li, Y. Chang, T. T. Ye, Z. Gao and J. Yang, *Adv. Mater. Technol.*, 2024, **2024**, 2400386.

22 S. Cichosz, A. Masek and M. Zaborski, *Polym. Test.*, 2018, **67**, 342–348.

23 J. Min, Y. Song and W. Gao, *Nat. Electron.*, 2022, **5**, 717–718.

24 L. Fan, W. Zheng, J. Xu and G. Yin, *Sens. Actuators, A*, 2023, **364**, 114823.

25 J. Huang, A. Chen, S. Han, Q. Wu, J. Zhu, J. Zhang, Y. Chen, J. Liu and L. Guan, *Adv. Sci.*, 2023, **10**, 2301116.

26 Y. J. Moon and K.-T. Kang, *Flexible Printed Electron.*, 2022, **7**, 024003.

27 R. Seghir and S. Arscott, *Sens. Actuators, A*, 2015, **230**, 33–39.

28 A. Kalra, A. Lowe and A. M. Al-Jumaily, *J. Mater. Sci. Eng.*, 2016, **5**, 1000254.

29 M. Kanungo, S. Mettu, K.-Y. Law and S. Daniel, *Langmuir*, 2014, **30**, 7358–7368.

30 X. Wang, H. Li, T. Wang, X. Niu, Y. Wang, S. Xu, Y. Jiang, L. Chen and H. Liu, *RSC Adv.*, 2022, **12**, 14190–14196.

31 I. S. Babichuk, C. Lin, Y. Qiu, H. Zhu, T. T. Ye, Z. Gao and J. Yang, *RSC Adv.*, 2022, **12**, 27687–27697.

32 Y. Bu, T. Shen, W. Yang, S. Yang, Y. Zhao, H. Liu, Y. Zheng, C. Liu and C. Shen, *Sci. Bull.*, 2021, **66**, 1849–1857.

33 H.-C. Lu and Y.-C. Liao, *Nanomaterials*, 2021, **11**, 2583.

© 2024 The Author(s). Published by the Royal Society of Chemistry